Road Curb Detection using 3D Lidar and Integral Laser Points for Intelligent Vehicles

Wentao Yao[1], Zhidong Deng[1,2] and Lipu Zhou[1]

***Abstract*—Road curb detection and tracking is essential for the autonomous driving of intelligent vehicles on highways and urban roads. In this paper, we present a fast and robust road curb detection algorithm using 3D lidar data and Integral Laser Points (ILP) features. Range and intensity data of the 3D lidar is decomposed into elevation data and data projected on the ground plane. First, left and right road curbs are detected for each scan line using the ground projected range and intensity data and line segment features. Then, curb points of each scan line are determined using elevation data. The ILP features are proposed to speed up the both detection procedures. Finally, parabola model and RANSAC algorithm is used to fit the left and right curb points and generate vehicle controlling parameters. The proposed method and feature provide fast and reliable road curb detection speed and performance. Experiments show good results on various highways and urban roads under different situations.**

I. Introduction

One of the key tasks for intelligent vehicles is to perform robust environment perception. For the autonomous driving of intelligent vehicles on highways and urban roads, the detection of road boundaries, namely curbs, is important and essential. Laser scanners, or lidars, have been widely used for this task, as their high resolution and wide field of view. Also, they are active sensors that can provide direct distance and intensity measurements, which are not interfered by weather, illumination and shadow. Passive sensors such as cameras, can also be used to detect road curbs, but the images are often influenced by lighting and shadow, which makes it hard to distinguish road curb pixels from other pixels. Also, distance measurements cannot be directly obtained in images. The advantages of lidars make them more accurate and stable than cameras in the road curb detection task.

Most reported lidar based road curb detection systems employ 2D lidars, which means the scanning is performed along a plane with a limited field of view (usually less than 180°). Each scanning acquires a range and angle sequence. Although the detection becomes faster with only a few measurements in each scanning, the detection of road curb will be more difficult as there are very few measurements belonging to a short segment of road curbs in a single scanning period.

*This work was supported in part by National Natural Science Foundation of China (NSFC) under grant No.90820305 and No.60775040.

[1,2]State Key Laboratory of Intelligent Technology and Systems, Tsinghua National Laboratory for Information Science and Technology, Department of Computer Science and Technology, Tsinghua University, Beijing 100084, China. Email: ywt@mails.tsinghua.edu.cn, michael@tsinghua.edu.cn, zlp09@mails.tsinghua.edu.cn

[2]Corresponding author

3D lidars have been introduced in recent years and develops rapidly. Rather than only one scanning plane, a 3D lidar contains a large number of scanning planes, resulting in a cloud of 3D points of distances and intensities during a single scanning period. This allows a good approximation of real 3D environments and make it easier to detect road curbs as there is a large number of lidar points on road curbs. Besides, a long segment of road curbs can be obtained in a single scanning period. However, vast amount of points poses a great challenge on the curb detection algorithm.

In this paper, we focus on the problem of road curb detection for intelligent vehicles on highways and urban roads with curbs of about 10-15cm high that separate the road surface from sidewalks or parkways. We propose a method that robustly detect road curbs in real-time. The major contribution of this paper are: First, we divide 3D lidar data into elevation data and ground projected data and detect road curb points on these two set of data respectively. Second, we propose the ILP feature to speed up the detection procedure. Third, range and intensity information of laser points are fused in the detection stage, which makes the results more accurate. Finally, parabola model and RANSAC algorithm are applied to model the shape of road curbs and compute vehicle controlling parameters for autonomous driving. Experimental results show good performance of our system on both highways and urban roads under different road situations, even on smoothly bent or non-flat road surfaces.

The paper is organized as follows. In Section II, some representative work for road curb detection is outlined. Section III describes the proposed ILP features, followed by the detailed description of the detection algorithm in Section IV. In Section V, we present some experimental results. Finally, Section VI concludes this paper and gives some future work.

II. Related Work

Many road boundary detection algorithms and systems have been developed over decades of years, including some road surface detection algorithms, which can also be used to detect road boundaries. In this section, we use word "boundary" to denote all types of road boundaries which divide road into traversable (road surface) and non-traversable (sidewalk, parkway, etc.) areas, not only road curbs.

Although some systems used camera as sensor [1] [2], most other systems employed 2D lidar sensors to detect road boundaries [3]. Since a 2D lidar has only one scanning plane, which means only a short segment of road boundaries at a certain distance can be obtained in a scanning period, the

978-1-4673-2743-5/12/$31.00 ©2012 IEEE

road boundary detection algorithms are often combined with GPS/IMU and odometry information to project successive frames of detection result into a same coordinate frame. When the vehicle moves, road boundaries can be modeled and tracked using Kalman filtering [4] [5] [6]. Applying lidar to road boundary detection was first introduced in [4]. They proposed an extended Kalman filtering based method for fast detection and tracking of road curbs using measurements obtained from a scanning 2D lidar. A method that combined elevation signals and signals projected on the ground plane in a two-stage manner to detect road and road-edge was presented in [7], which was fast and reliable. An interacting multiple model method that determine the existence of a curb based on a probability threshold and estimate the roadside curb position accurately was proposed in [6].

In recent years, 3D lidars are introduced and developed quickly. An obvious advantage of road boundary detection using 3D lidar is that the entire road boundary within a long range can be detected and modeled in a single scanning period. Also, the detection is more accurate according to the continuity between adjacent scanning lines. A 3D lidar was built using two 2D lidars rotated around a vertical axis to detect road curbs and intersections in [8]. Although the system was cheap, the slow rotation frequency made it difficult for real-time applications. A Velodyne 3D lidar, which is the same with ours, was used with a fast graph-based approach to segment ground and objects based on local convexity measures in [9]. As far as we know, we are the first to detect road curbs using a real 3D lidar.

Besides the above systems that made use of single sensor, some systems detected lane marking and road boundary based on camera and lidar sensor fusion [10] [11] [12] [13]. The fusion of lane marking and road boundary information will make the navigation of intelligent vehicles more reliable.

III. 3D LIDAR AND ILP FEATURE

In our road curb detection system, a Velodyne HDL-64E S2 3D lidar is mounted on the top of our intelligent vehicle THIV-II. It consists of 64 single lasers on a column. It rotates at a rate of 10Hz to provide a 360° field of view, and covers a pitch angle ranging from +2° to -24.8°. The angular resolution is 0.09°. It produces about 130,000 measurements in a single scanning. Each measurement, or point, consists of position (x, y, z), intensity I, scanning line order c (1-64), distance d and rotation angle $\theta \in (-180°, 180°]$ with $\theta = 0$ right in front of the vehicle. Raw points transmitted from the lidar are ordered by scanning line order c, and in each scanning line, points are in ascending order according to rotation angle θ, which is suitable in computing ILP features. Fig. 1 shows the THIV-II intelligent vehicle and the Velodyne 3D lidar, together with a typical image on real road captured by camera and the corresponding 3D points by the Velodyne 3D lidar. All objects in 360° field of view are explicitly expressed by these 3D points.

In order to speed up the detection, we first introduce the ILP features of each scanning line which are fast in computing the

(a) THIV-II and Velodyne 3D lidar

(b) Image of a typical road scene

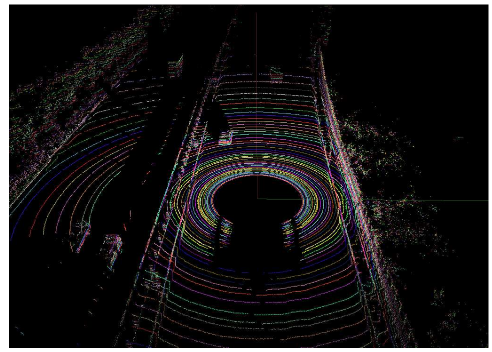

(c) 3D lidar points of the road scene in (b)

Fig. 1. THIV-II and a road scene expressed under camera image and Velodyne 3D lidar

sum of the 3D point features in a window of the scanning line. Since points in each scanning line are in ascending order of θ, we define some ILP features in Eq.(1)

$$\begin{aligned} I_x(i) &= \sum_{j=1}^{i} x_j \quad I_y(i) = \sum_{j=1}^{i} y_j \\ I_z(i) &= \sum_{j=1}^{i} z_j \quad I_{x^2}(i) = \sum_{j=1}^{i} x_j^2 \\ I_{y^2}(i) &= \sum_{j=1}^{i} y_j^2 \quad I_{xy}(i) = \sum_{j=1}^{i} x_j y_j \end{aligned} \tag{1}$$

where j is the index for each point in a scanning line and i is the index for ILP features; x, y, z stands for the coordinate of each point j.

When a new frame of lidar points received, the ILP features for all scanning lines can be calculated before the detection stage. It requires only one scan of all the points to get all the above ILP features. All the ILP features can be computed iteratively. For example, $I_x(i)$ can be computed as in Eq.(2), and the same with other ILP features.

$$I_x(i) = \sum_{j=1}^{i-1} x_j + x_i = I_x(i-1) + x_i \tag{2}$$

As mentioned above, the points in each scanning line are in ascending order of the rotation angle θ, this further reduce the computation in ILP features. Since only points in front of the vehicle will be taken into consideration, we only compute ILP features for points with $-90° \leq \theta \leq 90°$, which needs only half the computation for all points.

IV. Road curb detection using 3D lidar

In this section, we propose our road curb detection algorithm. Our algorithm consists of two stages. First, we project all lidar points onto the ground plane (x-y plane) by removing their z coordinates and detect road curbs using line segment features. Then, we consider elevation data to detect road curbs by height variation in z direction. Final curb points are the union of the detected curb points in these two stages.

A. Curb Detection on x-y Plane

Fig.2 is a simple model of one scanning line projected onto the x-y plane. Blue points are points on the road surface while yellow points are that on the curb. Red points are unidentified points which are outside the curbs, such that on the sidewalks, and will not be further considered in the curb detection task.

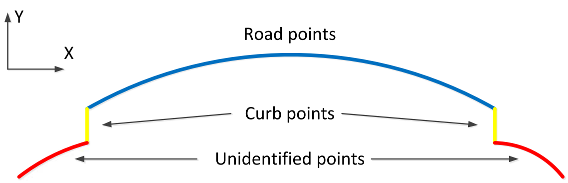

Fig. 2. Model of points in a single scanning line

We consider scanning lines separately. For points in each scanning line, we apply a sliding window containing N points and moving from center to sides. In each sliding window, the best linear fit and maximum difference between point intensities are calculated. The parameters for a linear fit $x = a_i y + b_i$ in window i is expressed in Eq.(3)

$$\begin{aligned} a_i &= \frac{\sum_{j=i+1}^{i+N} y_j \sum_{j=i+1}^{i+N} x_j - N \sum_{j=i+1}^{i+N} x_j y_j}{(\sum_{j=i+1}^{i+N} y_j)^2 - N \sum_{j=i+1}^{i+N} y_j^2} \\ b_i &= \frac{\sum_{j=i+1}^{i+N} y_j \sum_{j=i+1}^{i+N} x_j y_j - \sum_{j=i+1}^{i+N} y_j^2 \sum_{j=i+1}^{i+N} x_j}{(\sum_{j=i+1}^{i+N} y_j)^2 - N \sum_{j=i+1}^{i+N} y_j^2} \end{aligned} \tag{3}$$

By using the ILP features, Eq.(3) can be directly computed without calculating the sum of the points in the window. For example: $\sum_{j=i+1}^{i+N} y_j^2 = I_{y^2}(i+N) - I_{y^2}(i)$.

Given the best linear fit $x = a_i y + b_i$, the error is then expressed as Eq.(4)

$$\begin{aligned} d_i &= \sum_{j=i+1}^{i+N} (x_j - (a_i y_j + b_i))^2 \\ &= \sum_{j=i+1}^{i+N} x_j^2 - 2a_i \sum_{j=i+1}^{i+N} x_j y_j + a_i^2 \sum_{j=i+1}^{i+N} y_j^2 \\ &\quad -2b_i \sum_{j=i+1}^{i+N} x_j + 2a_i b_i \sum_{j=i+1}^{i+N} y_j + N b_i^2 \end{aligned} \tag{4}$$

Similarly, all the sums in Eq.(4) can be directly obtained by the ILP features. As adjacent sliding windows overlaps, lots of computation can be saved by using the ILP features instead of calculating the sums of points in each window.

In order to detect left and right curbs, two sliding window moves clockwise and anti-clockwise point by point respectively from the position where $\theta = 0$. Points in window i belongs to curb points if the following requirements are all satisfied:

- the linear fit has a small slope: $\|a_i\| < T_a$ (vehicle runs nearly parallel to curbs),
- the linear fit has a small error: $d_i < T_d$ (points belonging to curb should be on a line),
- intensity values in the window are different: $I_{max} - I_{min} > T_i$.

where T_a, T_d and T_i are threshold for slope, error and intensity difference, respectively.

For each scanning line, if a point does not belong to curb, we mark it as road points. Once a point belonging to curb is detected, we mark all the points in that window as curb points and put them to a set P_l or P_r (left or right curb) as candidate global curb points, and mark all remaining outside points as unidentified points. Then we move to the next scanning line and reset the sliding window to the center.

Although we focus on the problem of detecting road curbs, road boundaries are not always identified by curbs or other curb-like objects (guardrails or walls). Sometimes road boundaries are only white lines or grass. In these situations, intensity values of laser beams are particularly important. In our system, intensity values also help because the roads and sidewalks always have different intensity values. If the intensity values in the sliding window are different, it is probably that the window is crossing the curb area.

Fig.3 shows the detection result of three adjacent scanning lines. We set $N = 6$, $T_a = 0.2$, $T_d = 0.001\text{m}^2$ and $T_i = 10$. The color of the points are same with that in Fig.2. Points that belong to road and curbs are correctly detected and marked. The points outside the left curb are compacted because there is a slope on the left sidewalk, which makes the projected lidar points move rightward.

B. Curb Detection Using Elevation Data

The next stage for road curb detection is to make use of the elevation data (z coordinates of the lidar points) to distinguish curb points from road points. In real road circumstances, road surfaces are often smoothly bent, which makes it difficult to model the entire road surface as a plane. In addition, the sidewalks are often planar and only about 10-15cm above the road surface. The road surface and sidewalks will often be connected together and form a single plane, if we fit a best plane as road surface from points that may lies on road surface. In order to find curb points using elevation data, we still employ the sliding windows method and detect curb points scanning line by scanning line.

For each scanning line, a sliding window containing M points moves from center ($\theta = 0$) to sides. In each sliding

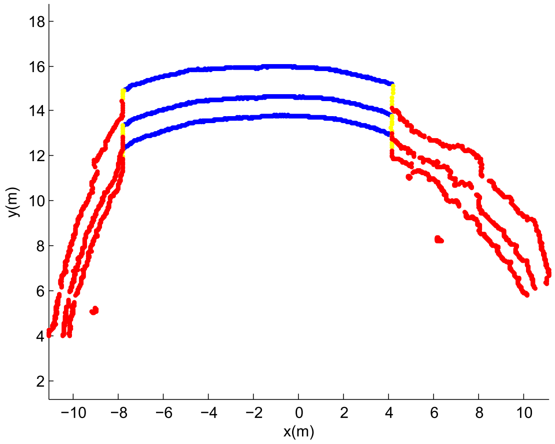

Fig. 3. Curb detection result of adjacent scanning lines on x-y plane

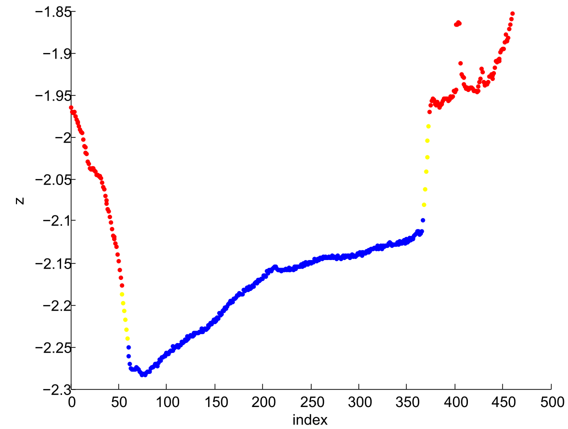

Fig. 4. Curb detection result of a scanning line using elevation data

window, we compare the average elevation of the points and the elevation of the last point. If the elevation of the last point is higher than the average elevation of the window to a threshold T_h, the last point is marked as a candidate curb point. If there is no candidate curb point in the next sliding window, the previous candidate points are regarded as false alarms and are removed from candidate curb point set. If there exists at least L successive candidate curb points, the curb is thought of found and all previous candidates are added to the global candidate curb points set P_l or P_r.

The ILP features is also helpful in computing the average elevation in the sliding windows. For window i, we have the average elevation H_i as:

$$H_i = \frac{1}{M}\sum_{j=i+1}^{i+M} z_i = \frac{1}{M}(I_z(i+M) - I_z(i)) \tag{5}$$

Fig.4 is the elevation data of a scanning line and the curb detection result. We set $M = 20$, $L = 6$ and $T_h = 0.03$m. The left and right curb are correctly detected and marked as yellow points. The color of the points are same with that in Fig.2. Besides, we can find the right side of the road is a curb, but the left side is a slope without obvious curb, the algorithm can still identify the boundary of road surface. In addition, the road surface (blue points) is smoothly bent, but this has no effect on our algorithm to detect the correct curbs.

C. Road Curb Model Fitting

The proposed algorithm described above is based on single scanning lines and the detected curbs for each scanning line can only describe a short segment of the entire curbs. Therefore, to describe entire curbs, a global curb model should be introduced to fit these local curb segments and parameterize the curbs. Vehicle controlling parameters for autonomous driving can also be generated from the curb model. For the highways and urban roads, we find the parabola model suitable for this task [14], which is expressed as $x = a_l y^2 + b_l y + c_l$ for left curb and $x = a_r y^2 + b_r y + c_r$ for right curb. Note that we do not impose parallelism on the left and right curb, as in some situations the left and right curbs are not parallel because of the changes in road width. Left and right curb model are fit from candidate points in P_l and P_r respectively. RANSAC algorithm is applied to remove outliers in P_l and P_r [15].

Fig.5 is the model fitting result for left and right curbs. The cyan and yellow points denotes for candidate curb points in P_l and P_r respectively. The red and blue curves indicate the fit curves for left and right curbs. The green curve is the target curve for the vehicle to track. In this scene, pedestrians and bicycles generate some false candidate curb points in front of the vehicle, but we could still get a good model fitting result.

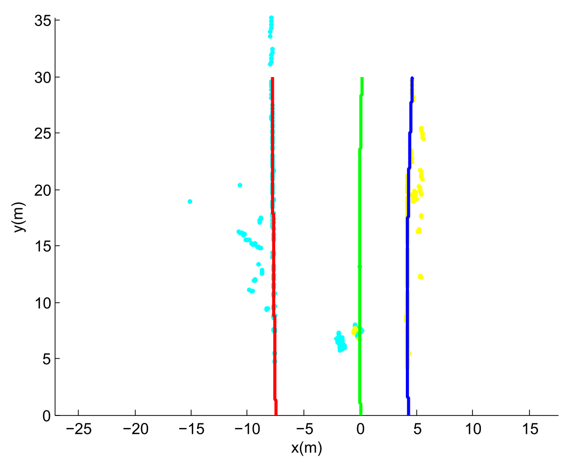

Fig. 5. Model fitting result for left and right curbs

For the autonomous driving of the intelligent vehicle, controlling parameters should be generated from the model. We first produce a target curve for the vehicle to track. The target curve is a linear combination of the left and right curbs, and is in the form of $x = a_t y^2 + b_t y + c_t$, where $\{a_t, b_t, c_t\} = (1-k)\{a_l, b_l, c_l\} + k\{a_r, b_r, c_r\}$, $k \in [0,1]$. k is the coefficient indicating the position of target curve. $k = 0.5$ means the target curve is the centerline of the road. The width of the road at the position of the vehicle can be approximated by $w = c_r - c_l$ if both curbs are fit well.

In the situation where only one side of the curbs can be successfully fit, we estimate another side of the curbs by current side and the width of the road. For example, if only the left curb is fit as $x = a_l y^2 + b_l y + c_l$, the right curb can thus be estimated as $x = a_l y^2 + b_l y + c_l + w$.

Given the target curve in vehicle coordinate frame, $x = a_t y^2 + b_t y + c_t$, we obtain a preview point on the curve in front of the vehicle. The distance from vehicle to preview point is in proportion to vehicle speed V and controlling interval T. The position and orientation of preview point in every frame is projected into a local navigation coordinate frame, and a parabola curve $f(y) = a_n y^2 + b_n y + c_n$ is again fitted using preview points of last several frames. The lateral offset X_L and yaw angle ψ from target curve in local coordinate frame to the vehicle at the preview distance can be computed:

$$\begin{aligned} X_L &= f(VT) = a_n(VT)^2 + b_n VT + c_n \\ \psi &= f'(VT) = 2a_n VT + b_n \end{aligned} \tag{6}$$

V. Experimental Results

In this section, we present some results of our curb detection system on real highways and urban roads. We first evaluated the performance of the proposed ILP features. Table.I lists the average processing time with and without using ILP features. "Ground" and "Elevation" means the detection on x-y plane and using the elevation data, as in Section IV. It is easy to find that detection with ILP features is much faster than that without ILP features. More computation can be saved using ILP features if N and L are larger.

TABLE I
Average processing time with and without ILP features (ms)

	Calculate ILP	Ground	Elevation	Fit	Total
with ILP	4	4	3	9	20
without ILP	0	12	9	9	30

Fig.6 shows some detection results on various road and under different road situations. Fig.6(a) was the detection result on a highway that is wide and with other vehicles that occludes some lidar points on curbs. Fig.6(b) was on an urban road with many other vehicles and bicycles. Although some detected curb points are far from the true curbs, we can still get a good result after model fitting. Fig.6(c) was on a curve urban road, showing good approximation of curbs by using the parabola model. In Fig.6(d), the vehicle was driving on a road that is narrowing. Curbs were not parallel in this situation but can still be correctly fit. Fig.6(e) was in the circumstance while there are pedestrians and bicycles in front of the vehicle. Besides, the ground was wet after raining, showing some "blank" areas on the road surface because the emitted laser was absorbed by water. Correct results could also be obtained in this situation. Finally, in Fig.6(f), several cars were parked at roadside and occlude most lidar points on the curb. Therefore, our algorithm regarded the boundary of these cars as curbs. This is not correct but reasonable, as the vehicle could not drive outside this "curb". Therefore, the boundary made by these cars should also be considered as the curb of the road. Since we do not have a 2D lidar that mostly used by other systems, the comparison with other road curb detection systems becomes very difficult.

VI. Conclusion and Future Work

In this paper, we present a fast and robust road curb detection algorithm using 3D lidar data and Integral Laser Points (ILP) features. Our algorithm is the fusion of the detection on the ground projected data and on elevation data. The ILP features are proposed to speed up the both detection procedures. Finally, parabola model and RANSAC algorithm is used to fit the left and right road curb points and generate vehicle controlling parameters. The proposed algorithm and feature provide a fast and reliable way for road curb detection task of intelligent vehicles. In future, fusion with camera-based lane marking detection and tracking results will be explored to get a more accurate road model.

References

[1] S.-j. Tsai and T.-y. Sun, "The Robust and Fast Approach for Vision-based Shadowy Road Boundary Detection," in *2005 IEEE Intelligent Transportation Systems*, 2005, pp. 79–84.

[2] J. Siegemund, U. Franke, and F. Wolfgang, "A Temporal Filter Approach for Detection and Reconstruction of Curbs and Road Surfaces based on Conditional Random Fields," in *IEEE Intelligent Vehicles Symposium*, no. Iv, 2011, pp. 637–642.

[3] C. Yu and D. Zhang, "Road Curbs Detection Based on Laser Radar," in *2006 8th International Conference on Signal Processing*, 2006, pp. 16–20.

[4] W. S. Wijesoma, K. R. Kodagoda, and A. P. Balasuriya, "Road-boundary detection and tracking using ladar sensing," in *IEEE Transactions on Robotics and Automation*, vol. 20, no. 3, Jun. 2004, pp. 456 – 464.

[5] S.-h. Kim, C.-w. Roh, S.-c. Kang, and M.-y. Park, "Outdoor Navigation of a Mobile Robot Using Differential GPS and Curb Detection," in *Robotics and Automation, 2007 IEEE International Conference on*, no. April, 2007, pp. 3414–3419.

[6] Y. Kang, C. Roh, S.-b. Suh, and B. Song, "A Lidar-Based Decision-Making Method for Road Boundary Detection Using Multiple Kalman Filters," *Industrial Electronics, IEEE Transactions on*, vol. 59, no. 11, pp. 4360–4368, 2012.

[7] W. Zhang, "LIDAR-based road and road-edge detection," in *IEEE Intelligent Vehicles Symposium*, 2010, pp. 845–848.

[8] F. Maurelli, D. Droeschel, T. Wisspeintner, S. May, and H. Surmann, "A 3D laser scanner system for autonomous vehicle navigation," in *International Conference on Advanced Robotics*, 2009, pp. 1–6.

[9] F. Moosmann, O. Pink, and C. Stiller, "Segmentation of 3D lidar data in non-flat urban environments using a local convexity criterion," in *IEEE Intelligent Vehicles Symposium*. Ieee, Jun. 2009, pp. 215–220.

[10] W. S. Wijesoma, K. R. Kodagoda, A. P. Balasuriya, and E. K. Teoh, "Road edge and lane boundary detection using laser and vision," in *IEEE/RSJ International Conference on Intelligent Robots and Systems*, vol. 3, 2001, pp. 1440–1445.

[11] A. S. Huang and S. Teller, "Lane Boundary and Curb Estimation with Lateral Uncertainties," in *IEEE/RSJ International Conference on Intelligent Robots and Systems, 2009. IROS 2009.*, 2009, pp. 1729–1734.

[12] J. Byun and M. C. Roh, "Autonomous Navigation of Transport Robot in the Urban Environment," in *2010 15th International Conference on Methods and Models in Automation and Robotics (MMAR)*, 2010, pp. 76–81.

[13] C. Chun, T.-b. Kwon, S. Suh, and S. Kang, "Autonomous Urban Navigation and Its Application to Patrol," in *2010 IEEE Workshop on Advanced Robotics and its Social Impacts (ARSO)*, 2010, pp. 46–51.

[14] K. Kluge, "Extracting road curvature and orientation from image edge points without perceptual grouping into features," in *Proceedings of the Intelligent Vehicles '94 Symposium*, 1994, pp. 109–114.

[15] M. A. Fischler and R. C. Bolles, "Random sample consensus: a paradigm for model fitting with applications to image analysis and automated cartography," *Commun. ACM*, vol. 24, no. 6, pp. 381—-395, 1981.

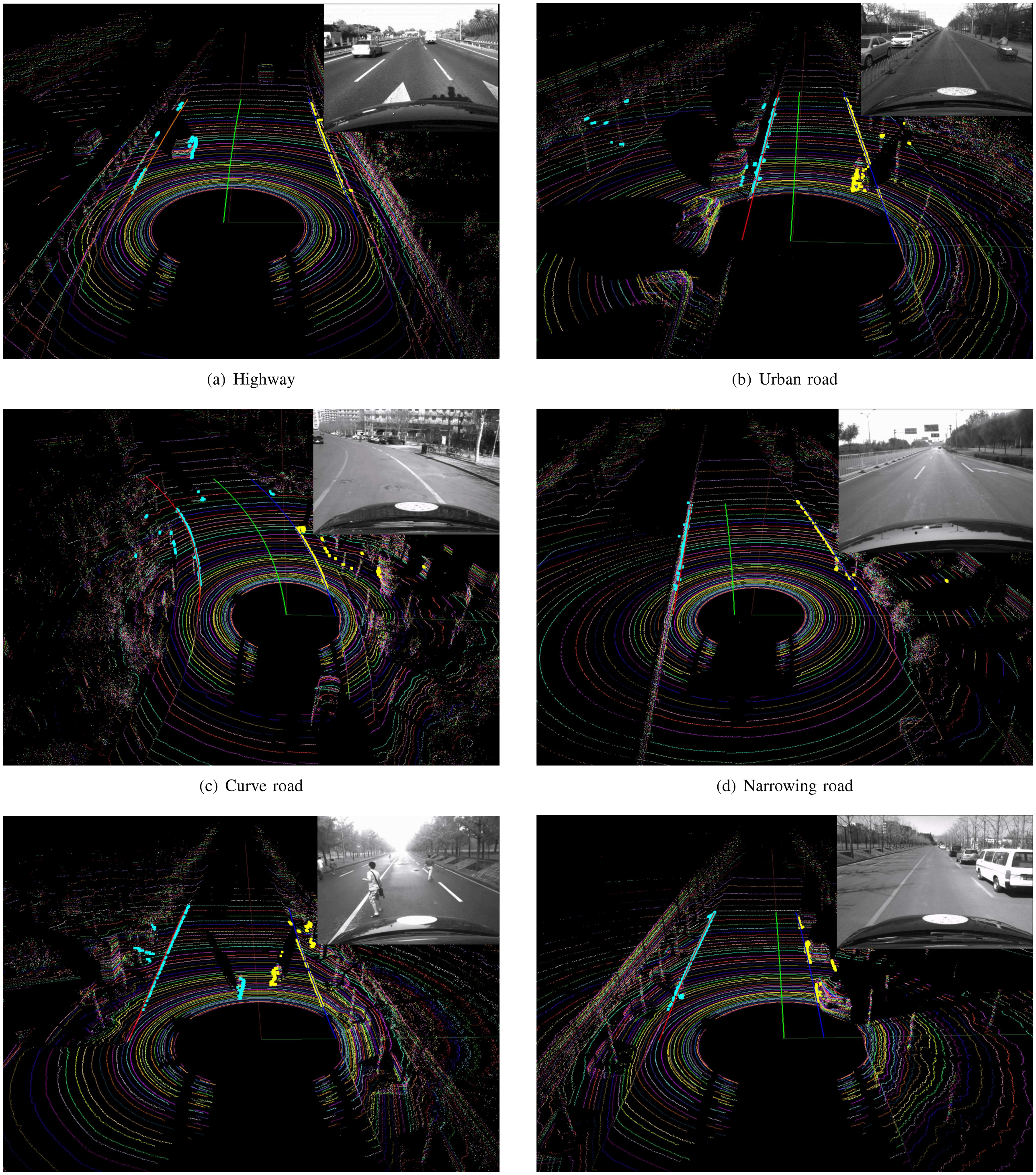

(a) Highway

(b) Urban road

(c) Curve road

(d) Narrowing road

(e) Obstructed by objects and water

(f) Parked cars at roadside

Fig. 6. Detection results under different road situations and corresponding image on the top-right corner (best viewed in color)